2023년 2월

박사학위 논문

Compensatory Inhibition of Osteoclastogenesis Against RANK by LGR4-involved Signaling Cascade

조 선 대 학 교 대 학 원

의 학 과

이 현 준

Compensatory Inhibition of Osteoclastogenesis Against RANK by LGR4-involved Signaling Cascade

파골세포에서 LGR4 신호 전달에 의한

RANK의 보상적 저해

2023년 2월 24일

조 선 대 학 교 대 학 원

의 학 과

이 현 준

Compensatory Inhibition of Osteoclastogenesis Against RANK by LGR4-involved Signaling Cascade

지도교수 손 홍 문

이 논문을 의학 박사학위신청 논문으로 제출함

2022년 10월

조 선 대 학 교 대 학 원

의 학 과

이 현 준

이현준의 박사학위 논문을 인준함

위원장 조선대학교 교수 이 준 영 (인)

위 원 조선대학교 교수 김 동 휘 (인)

위 원 전남대학교 교수 서 형 연 (인)

위 원 조선대학교 교수 임 원 봉 (인)

위 원 조선대학교 교수 손 홍 문 (인)

2023년 1월

조 선 대 학 교 대 학 원

CONTENTS

LIST OF FIGURES

ABSTRACT

파골세포에서 LGR4 신호 전달에 의한 RANK의 보상적 저해

이 현 준

지도교수 : 손 홍 문

조선대학교 대학원 의학과

목적: 파골세포의 발달 동안 receptor-activated nuclear factor kappa B (RANK)와 리간드 (RANKL)의 결합은 골다공증 치료제 개발의 중요한 표적으로 여겨진다. 최근에, leucine rich repeat containing G protein coupled receptor 4 (LGR4)는 파골세포 분화 동안 RANK 신호전달을 억제하는 RANKL-RANK 신호전달의 억제 조절자이며, 이의 작용제는 파골세포 생성 및 골다공증 치료를 위한 후보 물질로서 기대되고 있다. 본 연구에서는 RANKL 복합체의 결정 구조를 기반으로 제작된 RANKL 유래 돌연변이 RANKL(MT RANKL)을 도입하여 MT RANKL이 LGR4/AKT/GSK-3β 하위의 신호 조절이 RANK 신호 전달 없이 골수 유래 대식세포(BMM)에서 파골세포 생성을 억제할 수 있는지 여부를 조사하였다.

대상 및 방법: RANK/LGR4와 WT RANKL/MT RANKL 사이의 결합 친화도를 MST를 통해 분석하였고 AKT/GSK-3β/NFATc1 신호 전달을 Western Blot과 Confocal Microscopy를 통하여 분석하였다. 또한, RANKL-유도 골다공증 실험모델 마우스에서 LGR4의 면역양성 발현 및 LGR4 및 MT RANKL의 Co-localization을 분석하였

다.

결과: MT RANKL은 WT RANKL 대비 LGR4 결합 친화도는 유지되었고, AKT 인산화를 감소시키고 GSK-3을 증가시켜 파골세포 전구체 세포에서 NFATc1 전위를 억제하였다. 또한, MT RANKL은 RANKL로 유도된 마우스에서 LGR4의 발현을 촉진하였고, LGR4와의 Co-localization이 관찰되었으며, 효과적으로 골 흡수를 억제하는 것으로 나타났다.

결론: RANKL 유래 MT RANKL이 RANKL의 보상적 억제를 통해 RANKL 유도 파골세포 형성을 억제함으로써 새로운 골다공증 치료제로서의 가능성을 검증하였다.

색인단어: leucine rich repeat containing G protein coupled receptor 4(LGR4), Receptor activator of nuclear factor kappa B ligand(RANKL), 파골세포, 골다공증

I. INTRODUCTION

The receptor activator of nuclear factor kappa B ligand (RANKL) is an necessary cytokine that regulates osteoclastogenesis and function.[1)] Signals that determine the proliferation, differentiation, and function of cells of this lineage dictate the degree of skeletal remodeling.[2)] Various types of pharmaceutical agents have been introduced for osteoporosis, such as bisphosphonates, estrogen, and denosumab.[3-5)] However, recent bone-modeling agents have serious side effects sufficiently in order to reduce fracture susceptibility.[6)] Therefore, the development of agents that minimize bone resorption may be beneficial in the treatment of osteoporosis. Denosumab is a monoclonal antibody against RANKL that blocks its binding to RANK, thereby inhibiting the differentiation and activity of the osteoclasts, followed by the suppression of osteoporosis and other bone-related disorders.[78)] However, its side effects, which inhibit bone turnover and may lead to jaw necrosis.[9)] Recently, rebound resorption during the long-term or a discontinuous-taking period was reported as a side effect of denosumab.[10)]

Furthermore, the leucine rich repeat containing G protein coupled receptor 4 (LGR4) was introduced as another target for the inhibition of bone resorption as a compensation for RANK signaling during osteoclastogenesis.[11,12)13)] RANKL binding to LGR4 activates the Gαq and glycogen synthase kinase-3 β (GSK-3 β) signaling pathway. This pathway when inactivated upon RANKL stimulation is crucial for osteoclast differentiation during osteoclast development.[13-17)] This competes with RANK for RANKL binding in the osteoclast lineage cells.[18,19)] In

particular, in severe pathological states of the bone environments such as osteoporosis, LGR4 expression has shown a significant increase, suggesting that LGR4 target therapy may be an ideal choice for the recovery of the bone remodeling balance.

In a previous study, we developed a specific modified mutant RANKL (MT RANKL) based on the wild type RANKL (WT RANKL) sequence that may bind to LGR4 as an agonist, and investigated whether the present novel RANKL variant could interact with LGR4. Treatment with the mutant-type RANKL (MT RANKL) in mice inhibited osteoclast differentiation and production significantly, suggesting crosstalk between RANKL, RANK and LGR4.[20,21] However, it is unclear whether MT RANKL can bind to LGR4, but not to RANK and whether it can inhibit osteoclastogenesis by inhibiting RANKL-RANK signaling and trigger downstream signaling pathways such as GSK3beta and AKT.

Therefore, in this study, the author aimed to demonstrate that when compared with WT RANKL (Wild type RANKL), MT RANKL binds to LGR4 instead of RANK and that, via this ligand, it acts to regulate the RANK signaling cascade in RANKL-induced osteoclast differentiation and bone remodeling, negatively. Finally, we aimed to determine whether the targeting of the LGR4 binding novel agonist could be a pharmacological approach for the treatment of osteoporosis.

II. MATERIALS AND METHODS

WT/ MT RANKL, RANK and LGR4 generation and purification

WT RANKL and MT RANKL were generated as described previously[22]. The genes encoding RANK and LGR4 were synthesized and codon-optimized. The cells were fragmented using ultra-sonification at 5℃. The RANK and LGR4 proteins were eluted with imidazole in C-P buffers.

Binding affinity measurement

The protein binding affinity was measured using microscale thermophoresis (MST).[23] The MST experiments were carried out using Monolith cells 115 (NanoTemper Technologies GmbH). After mixing WT/MT RANKL and RANK/LGR4, samples were incubated before loading into capillaries. To bind check, RANK/LGR4 or WT RANKL/MT RANKL was mixed with an equal volume. The samples were incubated for 1 h. The MST power to "medium" and intersection point was determined using the manufacturer's protocol.

Mice

Five-week-old female mice (BL-6; Orient Bio Co. LTD, Seoul, South Korea) were sacrificed for the *in vitro* and *in vivo* studies. All the experimental procedures involving animals were approved by the Institutional Animal Care and Use Committee (CIACUC2018-S0012-1) of the Chosun University, Gwangju, South Korea.

Primary Cell culture and in vitro Osteoclast Differentiation

The BMMs were obtained from the femurs by flushing the bones with α-MEM medium using previously described methods.[24] To generate OCs, BMMs (50,000/cm^2) were cultured in an α-MEM medium containing M-CSF and the indicated concentrations of WT RANKL.

RNA Interference

A custom SMART pool plus the small interfering RNA (siRNA) to target the mouse LGR4 (M-041080) was designed and synthesized by Dharmacon (Lafayette, CO). siRNA (10 nmol) and transfected into the BMMs using Lipofectamine TM 2000 (Invitrogen) according to the manufacturer's protocol. After transfection, the BMMs were cultured with M-CSF and RANKL for four days and then differentiated into osteoclasts.

Real-time reverse transcription PCR (RT-PCR) analysis

The RNA was extracted and the mRNA levels were measured using RT-PCR, and GAPDH was used as a control. Sequences of the primers used to current study were presented in a previous study.[21]

Western blot analysis

The protein samples was incubated at 4 °C with the appropriate primary antibodies, p-Akt (1:1,000; 9271S; Cell Signaling Technology), Akt (1:1,000;

9272S; Cell Signaling Technology), p-GSK-3β (1:1,000; 9336S; Cell Signaling Technology), GSK-3β (1:1,000; 9315S; Cell Signaling Technology), RANK (1:1,000; 4845S; Cell Signaling Technology), and LGR4 (1:500; MBS468030; MyBioSource).

III. RESULTS

Binding affinity between RANK/LGR4 and WT RANKL/MT RANKL

The ligand protein sequences of WT RANKL and MT RANKL are presented in Fig. 1a, and the receptor proteins, RANK and LGR4, in the extracellular domain for the ligand-binding assay are shown in Fig. 1b. WT RANKL was generated at the TNF homology domain in the soluble RANKL domain, and MT RANKL was transferred to K180R, D189I, R190K, H223F, and H224Y on the WT RANKL. The purified receptors were characterized using the western blot analysis for the Histag band. The purified RANK and LGR4 were detected at 24Kda and 47Kda using the same Histag bands.

To determine the binding affinity of WT RANKL or MT RANKL for RANK or LGR4, MST assays were carried out (Fig. 1c, 1d). The MST measurements showed an approximately 500 fold nanomolar binding affinity of WT RANKL for RANK, with a KD of 33.3±9.2nM while that of MT RANKL for RANK was 1.62 ± 0.057μM. On the other hand, there was no significant difference between the KD values of WT RANKL to LGR4, 409±24nM compared to that for MT RANKL to LGR4, 370±17nM.

These results showed that MT RANKL maintained a strong binding affinity for LGR4 and WT RANKL, but not with RANK, compared to the binding affinity of WT RANKL. This indicated that MT RANKL may stimulate the LGR4 signaling cascade without RANK signaling in the WT RANKL-induced signaling cascade.

Effect of MT RANKL on the RANK-RANKL/LGR4-RANKL signaling cascade

To investigate the effect of the WT RANKL-induced LGR4 signaling cascade on the inhibition of osteoclastogenesis by MT RANKL *in vitro*, the BMMs were treated with LGR4 siRNA (Fig. 2a). The knockdown of LGR4 expression was detected in the LGR4 siRNA-treated BMMs using the western blot technique, whereas the RANK expression was maintained (Fig. 2b).

The number and size of the BMMs that differentiated into mature, TRAP-positive, multinucleated osteoclasts were observed in the LGR4 siRNA-treated BMM (Fig. 2c). The MT RANKL decreased the number and size of the TRAP-positive cells in the control siRNA-treated BMM in the presence of WT RANKL. However, MT RANKL did not decrease the number and size of TRAP-positive cells in LGR4 siRNA-treated BMM in the presence of WT RANKL. In addition, the number of osteoclast cells decreased significantly in the WT RANKL + MT RANKL-treated BMMs in the presence of the Con siRNA (Fig. 2d). However, there was no effect on the presence of the LGR siRNA.

The expression of several osteoclast-specific genes in both WT RANKL-and WT RANKL + MT RANKL-treated BMMs using RT-PCR were investigated (Fig. 2e). Our results on day three post-treatment, showed a significant increase in TRAP, OSCAR, and the NFATc1 mRNA expression, which are known to be related to the differentiation and activity of osteoclasts in the mRANKL-WT + mRANKL-MT-treated BMMs.

Whether treatment with WT RANKL or MT RANKL for different durations led to the induction of AKT, Src, and GSK-3β phosphorylation by the RANK and LGR4 signaling cascades were investigated (Fig. 2f). In the LGR4 siRNA-treated BMMs,

WT RANKL treatment led to an obvious increase in Src and AKT phosphorylation and a decrease in GSK-3β. However, the MT RANKL treatment did not affect AKT and GSK-3β phosphorylation in the LGR4 siRNA-treated BMMs.

Overall, these results demonstrated that MT RANKL inhibits osteoclast differentiation and activity via the LGR4-dependent signaling pathway in contrast to the RANK signaling in the RANKL-induced BMMs.

Effect of MT RANKL on the AKT-induced signaling cascade

To evaluate the AKT-mediated LGR4 signaling cascade, WT RANKL or MT RANKL treatment on the AKT inhibitor, MK 2206-pretreated BMM was administered. Cell viability assays were performed to determine the optimal concentration of MK 2206 in the BMMs (Fig. 3a). The cell viability decreased in a dose-dependent manner with the MK 2206 treatment. The 0.2 μM MK 2206 did not affect the BMMs cell viability at the maximum concentration; therefore, further experiments were conducted using 0.2 μM MK 2206.

Treatment with WT RANK in the presence of MK 2206 was showed a significant decrease in the number of TRAP-positive multinuclear cells (Fig. 3b, 3c). However, MT RANKL treatment in the presence of MK 2206 had no effect on the BMMs.

Although a slight inhibitory effect of GSK-3β phosphorylation by WT RANKL in the presence of MK 2206 was detected in the BMMs (Fig. 3d), a total increase in the phosphorylation of GSK-3β by MT RANKL was observed in the MK 2206 pre-treated BMMs. In addition, a complete block of the phosphorylation of AKT was observed in both the WT RANKL-and MT RANKL-treated BMMs in the presence of

MK 2206. These results suggested that MT RANKL may lead to the phosphorylation of GSK-3β that is dependent on AKT, resulting in no effect on osteoclastogenesis alone.

Effect of MT RANKL on the GSK-3B-induced signaling cascade

To investigate the GSK-3β -mediated LGR4 signaling cascade, pretreatment with LiCl, a powerful GSK-3β inhibitor, was performed on the WT RANKL-or MT RANKL-treated BMMs. Cell viability assays were performed to determine the appropriate LiCL concentration. (Fig. 4a). As reported previously for MK 2206, cell viability decreased in a dose-dependent manner using LiCl. The concentration of 5mM LiCl did not affect the BMMs cell viability; therefore, further experiments were performed using 5mM LiCl.

The treatment of WT RANK in the LiCl pretreated BMMs led to a significant increase in the TRAP-positive multinuclear cells (Fig. 4b, 4c). However, MT RANKL had no effect on the BMMs in the presence or absence of LiCl.

In addition, a significant increase in GSK-3β phosphorylation with the pretreatment with LiCl in the presence of WT RANKL or MT RANKL was detected, although AKT was not changed (Fig. 4d). These results suggested that MT RANKL may transfer the signal in a manner dependent on the phosphorylation of GSK-3β in the BMM.

Effect of MT RANKL on NFATc1 translocation to the nucleus

To evaluate the effect of MT RANKL on LGR4 dependent inhibition of NFATc1

translocation to the nucleus, the nuclear and cytosolic localization of NFATc1 was examined using the western blot technique and a densitometric analysis in the con or LGR4 siRNA treated BMMs (Fig. 5a, 5b). Nuclear NFATc1 was detected and it showed a significant increase in the control siRNA with WT RANK-treated BMMs. However, in the LGR4 siRNA-treated BMMs, nuclear NFATc1 in the MT RANKL-treated BMMS in the presence of WT RANKL was not detected. In the confocal microscopic analysis, while NFATc1 was present in the nuclei of WT RANKL with the control siRNA-treated BMMs (Fig. 5c), it was not detected in the nuclei of the LGR4 siRNA-treated BMMS with WT RANKL + MT RANKL.

These results further supported our hypothesis that LGR4 signaling plays a critical role in the MT RNAKL induced inhibition of NFATc1 translocation to the nucleus in the WT RANKL-treated BMMs, suggesting that MT RANKL may be considered an effective compensative inhibitor for WT RANKL.

Effect of MT RANKL on RANKL-induced mice

To investigate the effect of MT RANKL on bone lysis, healthy mice were treated with MT RANKL in the presence or absence of WT RANKL, and their femur bones were examined using micro-CT (Fig. 6a). Mice in the WT RANKL-treated group exhibited significant bone loss, whereas those in the WT RANKL+ MT RANKL-treated group exhibited little bone loss. Mice in the MT RANKL-treated group showed no significant bone loss compared to those in the control group. The BV/TV and BMD were assessed using a quantitative micro-CT (Fig. 6b). As expected, the BV/TV and BMD showed a decrease in the WT RANKL-treated mice

and a significant recovery with MT RANKL treatment. These results demonstrated clearly, the therapeutic effects of MT RANKL in osteoporosis.

In addition, the immunopositive expression of RANK, LGR4 and NFATc1 were observed in the H&E-stained histological sections of the femur bone (Fig. 6c). The WT RANKL-treated mice showed a strong immunopositive expression of NFATc1, whereas the MT RANKL and WT RANK + MT RANKL-treated mice exhibited a lower NFATc1 expression. In addition, LGR4 expression increased slightly in the WT RANK + MT RANKL-treated mice.

Finally, a colocalized immunofluorescence of WT RANKL/MT RANKL and RANK/LGR4 was observed using confocal microscopy (Fig. 6d). WT RANKL was co-located in both RANK and LGR4, whereas MT RANKL was only present in LGR4.

Taken together, these results demonstrated that MT RANKL may inhibit RANKL-induced bone lysis in a mouse model via the LGR4-dependent compensational signaling pathway and may be a useful pharmaceutical agent in severe osteoporosis.

IV. DISCUSSION

Currently, it has been reported frequently that RANKL binds to its receptor RANK, drives the development of osteoclasts, and is considered to be a pivotal target protein.[25] After denosumab treatment have arisen recently. RANKL scavenging by denosumab leads to the repeated regeneration of RANKL, resulting in a more severe rebound bone resorption in patients with osteoporosis, than that before treatment.

Recently, LGR4 was reported as another receptor for RANKL with comparative binding to RANK, resulting in the negative regulation of RANKL-RANK signaling during osteoclastogenesis.[26] Moreover, previous studies showed that a novel RANKL mutant as an agonist of LGR4 may inhibit the differentiation and activation of osteoclasts in RANKL-induced osteoclastogenesis in *in vitro* and *in vivo* experimental models.[13] Thus, LGR4-agonist signaling was expected to inhibit NFATc1 signaling through the intracellular LGR4- GSK3-β signaling pathway in the RANKL-RANK binding-induced osteoclast progenitor cells, resulting in a block in osteoclast development.[13]

In this study, whether the MT RANKL derived from the RANK binding site changed RANKL with the TNFR11 homology domain, which was shown in a previous study to bind to LGR4 without binding to RANK were investigated.[21] MT RANKL changed the RANK binding domain in RANKL, to one with a similar amino acid composition, and maintained the LGR4 binding affinity; however, the RANK binding affinity decreased to 1/500 of that of WT RANKL-RANK. The minimal change in the RANK

binding domain in RANKL may maintain the RANKL homeostasis in the living body and not affect the additional RANKL release, resulting in a resolution of the rebound resorption after the discontinuation of the drugs used to treat osteoporosis.[13)]

In addition, in the mouse model, the colocalized MT RANKL was only observed with LGR4, whereas in WT RANKL it was RANK and LGR4. This indicates that WT RANKL may react with RANK and LGR4; however, MT RANKL only stimulated LGR4 in WT RANKL-induced osteoclastogenesis. Additional stimulation of LGR4 in the RANKL-induced osteoclast precursor cells may trigger a negative regulatory signal against RANKL-RANK, and the signaling cascade from LGR4 is expected to boost the NFATc1-related signaling.[27)] Another report showed that NFATc1 was responsible for driving the early differentiation and solidification of the osteoclast commitment osteoclast.[28)] The downregulation of RANK signaling it has been suggested that targeting AKT signaling promotes IκBα degradation, resulting in the translocation of NFATc1.[29,30)] Thus, signaling from LGR4-MT RANKL inhibited AKT phosphorylation and stimulated GSK3-β Ser9 phosphorylation, resulting in an inhibition of NFATc1 translocation independent of the RANK signaling cascade. In particular, MT RANKL signaling could not induce any stimulation of GSK3-β Ser9 phosphorylation and osteoclast development in the AKT-blocked BMM. MT RANKL not RANK, has been suggested as an effective LGR4 signaling trigger as an agonist. In another report, LGR4 expression was found to be induced resulting in RANKL-NFATC1 signaling during osteoclast differentiation.[31)]. This mechanism implies that LGR4 plays a critical role in osteoclast homeostasis by reducing the expression of the death receptors such as the Fas receptor. [32)33)] The present study implied that

LGR4 may be a pivotal player in the negative-feedback mechanism that controls the activity of osteoclasts. The LGR4 signaling cascade induced by MT RANKL inactivated AKT and activated the GSK-3β signaling pathway, which inhibits the activity of NFATC1 during osteoclast differentiation.

V. CONCLUSION

MT RANKL, a novel agonist of LGR4, induces a compensatory inhibitory effect on RANKL. Moreover, MT RANKL is involved in the LGR4-induced GSK3-β Ser9 phosphorylation mediated by the negative-feedback mechanism of osteoclast. Therefore, in this study, in RANKL-induced mice, MT RANKL induced phosphorylation of GSK-3β, as well as inhibited the NFATc1 translocation and bone resorption. Furthermore, this study demonstrated that MT RANKL is the potential role to be a useful tool for the treatment of osteoporosis by inhibiting the RANKL-induced bone resorption via the compensatory inhibition of the RANKL-RANK signaling cascade. Moreover, There was a lack of the side effects that are common in previous osteoporosis treatments, such as rebound resorption after discontinuation.

REFERENCES

1. Hofbauer LC, Kuhne CA, Viereck V. The OPG/RANKL/RANK system in metabolic bone diseases. J Musculoskelet Neuronal Interact. 2004;4:268-75.

2. Wang L, You X, Zhang L, Zhang C, Zou W. Mechanical regulation of bone remodeling. Bone Res. 2022;10:16.

3. Hanley DA, Adachi JD, Bell A, Brown V. Denosumab: mechanism of action and clinical outcomes. Int J Clin Pract. 2012;66:1139-46.

4. Gowen M, Stroup GB, Dodds RA, et al. Antagonizing the parathyroid calcium receptor stimulates parathyroid hormone secretion and bone formation in osteopenic rats. J Clin Invest. 2000;105:1595-604.

5. Martin TJ. Bone biology and anabolic therapies for bone: current status and future prospects. J Bone Metab. 2014;21:8-20.

6. Sozen T, Ozisik L, Basaran NC. An overview and management of osteoporosis. Eur J Rheumatol. 2017;4:46-56.

7. Miller PD. Denosumab: anti-RANKL antibody. Curr Osteoporos Rep. 2009;7:18-22.

8. Cadieux B, Coleman R, Jafarinasabian P, et al. Experience with denosumab (XGEVA(R)) for prevention of skeletal-related events in the 10 years after approval. J Bone Oncol. 2022;33:100416.

9. Pittman K, Antill YC, Goldrick A, Goh J, de Boer RH. Denosumab: Prevention and management of hypocalcemia, osteonecrosis of the jaw and atypical fractures. Asia Pac J Clin Oncol. 2017;13:266-76.

10. Anastasilakis AD, Makras P, Yavropoulou MP, Tabacco G, Naciu AM, Palermo A. Denosumab Discontinuation and the Rebound Phenomenon: A Narrative Review. J Clin Med. 2021;10

11. Jönsson B, Ström O, Eisman JA, et al. Cost-effectiveness of denosumab for the treatment of postmenopausal osteoporosis. Osteoporos Int. 2011;22:967-82.

12. Kostenuik PJ, Nguyen HQ, McCabe J, et al. Denosumab, a fully human monoclonal antibody to RANKL, inhibits bone resorption and increases BMD in knock-in mice that express chimeric (murine/human) RANKL. J Bone Miner Res. 2009;24:182-95.

13. Luo J, Yang Z, Ma Y, et al. LGR4 is a receptor for RANKL and negatively regulates osteoclast differentiation and bone resorption. Nat Med. 2016;22:539.

14. van Dam PA, Verhoeven Y, Jacobs J, et al. RANK-RANKL Signaling in Cancer of the Uterine Cervix: A Review. Int J Mol Sci. 2019;20:2183.

15. Matsumoto Y, Larose J, Kent OA, et al. RANKL coordinates multiple osteoclastogenic pathways by regulating expression of ubiquitin ligase RNF146. J Clin Invest. 2017;127:1303-15.

16. Kang IS, Kim C. NADPH oxidase gp91 phox contributes to RANKL-induced osteoclast differentiation by upregulating NFATc1. Scientific reports. 2016;6:38014.

17. Jang HD, Shin JH, Park DR, et al. Inactivation of glycogen synthase kinase-3beta is required for osteoclast differentiation. J Biol Chem. 2011;286:39043-50.

18. Yi H. Identification and Characterisation of Lgr4/β-catenin Signalling in Acute Myeloid Leukaemic Stem Cells. Published online 2016;

19. Renema N, Navet B, Heymann M-F, Lezot F, Heymann D. RANK-RANKL

signalling in cancer. Bioscience reports. 2016;36:e00366.

20. Ko Y, Lee G, Kim B, Park M, Jang Y, Lim W. Modification of the RANKL-RANK-binding site for the immunotherapeutic treatment of osteoporosis. Osteoporos Int. 2020;31:983-93.

21. Ko YJ, Sohn HM, Jang Y, et al. A novel modified RANKL variant can prevent osteoporosis by acting as a vaccine and an inhibitor. Clin Transl Med. 2021;11:e368.

22. Jang Y, Sohn HM, Ko YJ, Hyun H, Lim W. Inhibition of RANKL-Induced Osteoclastogenesis by Novel Mutant RANKL. Int J Mol Sci. 2021;22

23. Romain M, Thiroux B, Tardy M, Quesnel B, Thuru X. Measurement of Protein-Protein Interactions through Microscale Thermophoresis (MST). Bio Protoc. 2020;10:e3574.

24. Bartell SM, Kim HN, Ambrogini E, et al. FoxO proteins restrain osteoclastogenesis and bone resorption by attenuating H2O2 accumulation. Nat Commun. 2014;5:3773.

25. Cao X. RANKL-RANK signaling regulates osteoblast differentiation and bone formation. Bone Res. 2018;6:35.

26. Luo J, Zhou W, Zhou X, et al. Regulation of bone formation and remodeling by G-protein-coupled receptor 48. Development. 2009;136:2747-56.

27. Luo J, Yang Z, Ma Y, et al. LGR4 is a receptor for RANKL and negatively regulates osteoclast differentiation and bone resorption. Nat Med. 2016;22:539-46.

28. Lee Y, Kim HJ, Park CK, et al. MicroRNA-124 regulates osteoclast

differentiation. Bone. 2013;56:383-9.

29. Cong F, Wu N, Tian X, et al. MicroRNA-34c promotes osteoclast differentiation through targeting LGR4. Gene. 2017;610:1-8.

30. Moon JB, Kim JH, Kim K, et al. Akt induces osteoclast differentiation through regulating the GSK3beta/NFATc1 signaling cascade. J Immunol. 2012;188:163-9.

31. Wang M, Liu J, Zhu G, Chen X. Low levels of cadmium exposure affect bone by inhibiting Lgr4 expression in osteoblasts and osteoclasts. J Trace Elem Med Biol. 2022;73:127025.

32. Wu X, Pan G, McKenna MA, Zayzafoon M, Xiong WC, McDonald JM. RANKL regulates Fas expression and Fas-mediated apoptosis in osteoclasts. J Bone Miner Res. 2005;20:107-16.

33. Manolagas SC, Parfitt AM. What old means to bone. Trends Endocrinol Metab. 2010;21:369-74.

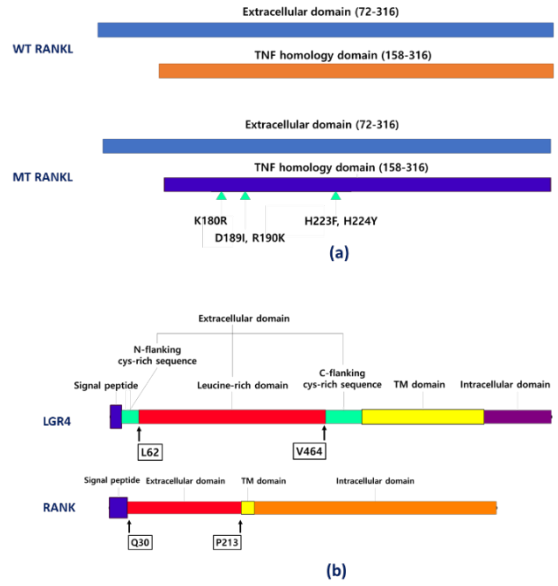

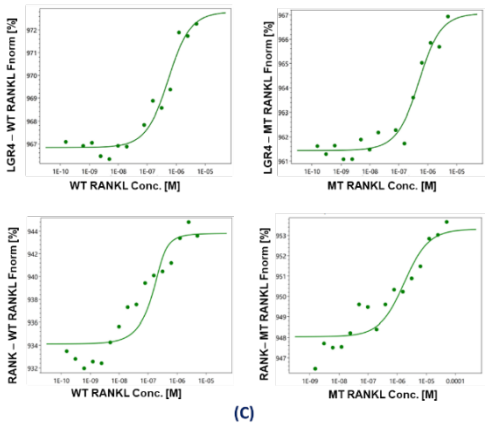

	Receptor Conc.	Kd	Signal to Noise Ratio
LGR4-WT RANKL	250nM	409±24nM	12.8
LGR4-MT RANKL	250nM	370±17nM	13.6
RANK-WT RANKL	250nM	33.3±9.2nM	6.3
RANK-MT RANKL	250nM	1.62±0.057μM	6.9

(d)

Figure 1. Suitability of microscale thermophoresis (MST) as a sensitive method to determine WT RANKL/MT RANKL binding affinities. (a) Protein sequences of WT RANKL and MT RANKL in present study. (b) Protein sequence of receptor protein LGR4 and RANK in present study. The receptor LGR4 sequence presents from L62 to V464 as extracellular domain as ligand binding and RANK from Q30 to P213. (c) The titration of WT RANKL/MT RANKL ranged from 11.5 nM to 50 μM with a constant concentration of the labelled receptor LGR4 and RANK at 250 nM. (d) Data present LGR4/RANK and WT RANKL/MT RANKL binding affinity as Kd values. Despite the small changes in the molecule's mass, a signal-to-noise ratio of 13.6 allows an accurate determination of the interaction strength. The error values represent the ± S.D. of each data point calculated from three independent thermophoresis measurements.

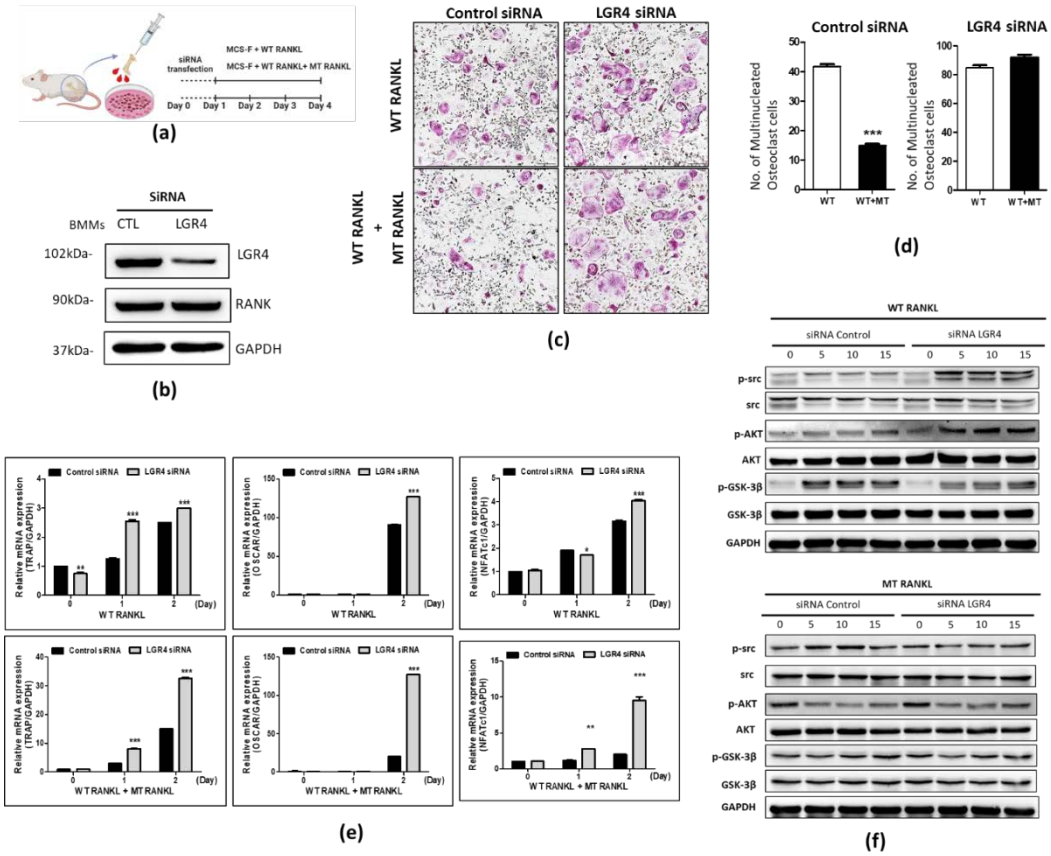

Figure 2. Effect of MT RANKL on osteoclast differentiation *in vitro* (a). Schedule for sampling in WT RANKL or WT RANKL + MT RANKL-treated BMM in presence with Control or LGR4 siRNA. (b) Western blot analysis of LGR4 and RANK in LGR4 siRNA treated BMMs. The significant decreased LGR4 expressions were detected in LGR4 siRNA treated BMMs. (c) A typical image of BMMs stained for TRAP (red) after treatment with WT RANKL (75 ng/mL) or WT RANKL (75 ng/mL) + MT RANKL (75 ng/mL) in Control siRNA or LGR4 siRNA treated BMMs. Magnifications are 100X. Size bar is 20 μm. (d). Numbers of multinucleated TRAP positive cells (≥3 nuclei) in these cultures (n = 3); (e). Osteoclast related gene expressions in Control siRNA or LGR4 siRNA treated BMMs. BMMs were exposed to WT RANKL

(75 ng/mL) or WT RANKL (75 ng/mL) + MT RANKL (75 ng/mL) for 2 days. Gene expression was determined by real-time PCR and normalized to the expression of GAPDH. The data come from three separate experiments and are expressed as the mean ± standard deviation (SD). *P < 0.01. (f) Western blot analysis of the RANK and LGR4 signaling cascades in Control siRNA or LGR4 siRNA treated BMMs in presence with WT RANKL (2 μg/mL) or MT RANKL (2 μg/mL). GAPDH was used as a loading control.

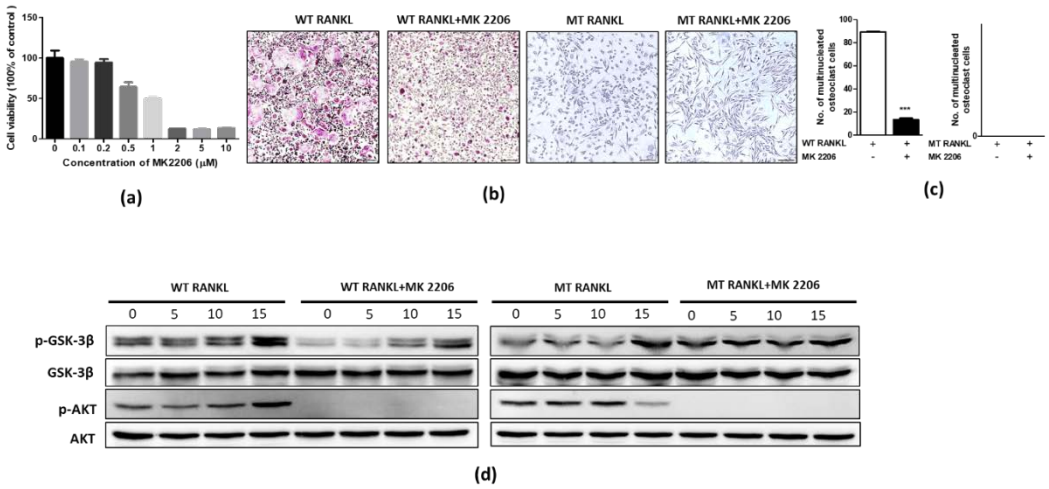

Figure 3. Effect of MT RANKL on the AKT-induced signaling cascade. (a) Cell viability was determined by 3-(4,5-dimethylthiazol-2-yl)-2,5-diphenyltetrazolium bromide (MTT) assay. BMMs cells were exposed to various doses of MK 2206. The results are presented as the mean ± standard deviation (SD) of three independent experiments. (b) TRAP stanning in presence with WT RANKL (75 ng/mL) or MT RANKL (75 ng/mL) in MK2206-pretreated BMM. The MK2206 were pretreated at 8hrs before RANKL treatment. Magnifications are 100X. Size bar is 20 μm. (c). Numbers of multinucleated TRAP positive cells (≥3 nuclei) in these cultures (n = 3), (d) Western blot analysis of the RANK and LGR4 signaling cascades. Results are representative of three separate experiments with comparable results. BMMs were exposed to WT RANKL (2 μg/mL) or MT RANKL(2 μg/mL) at various time intervals after 8hrs with or without MK2206 pretreatment.

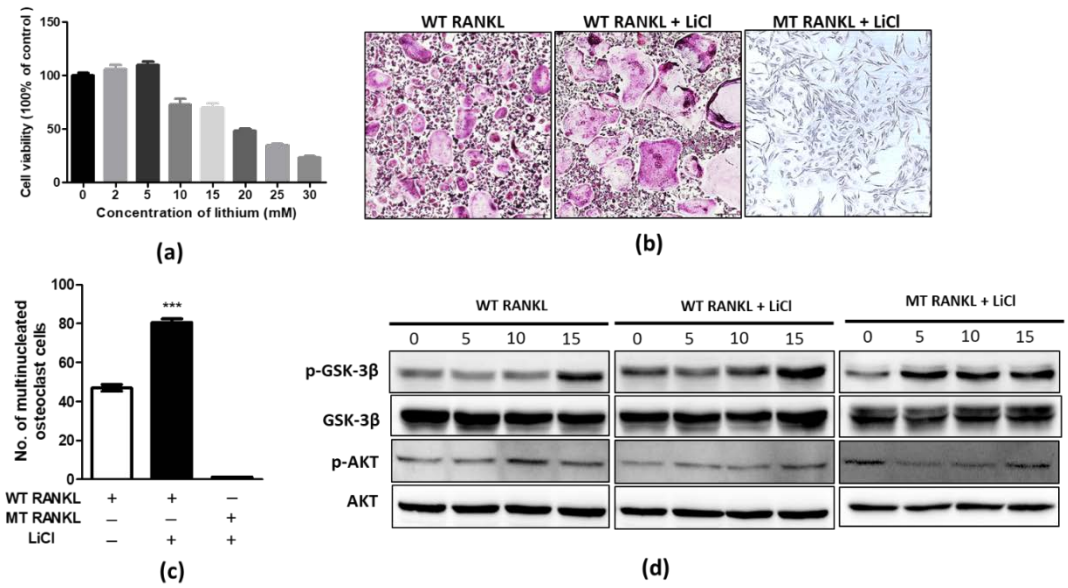

Figure 4. Effect of MT RANKL on the GSK-3β-induced signaling cascade. (a) Cell viability was determined by MTT assay. BMMs cells were exposed to various doses of LiCl. The results are presented as the mean ± standard deviation (SD) of three independent experiments. (b) TRAP stanning in presence with WT RANKL (75 ng/mL) or MT RANKL (75 ng/mL) in LiCl-pretreated BMM. The LiCl were pretreated at 8hrs before RANKL treatment. Magnifications are 100X. Size bar is 20 μm. (c). Numbers of multinucleated TRAP positive cells (≥3 nuclei) in these cultures (n = 3), (d) Western blot analysis of the RANK and LGR4 signaling cascades. Results are representative of three separate experiments with comparable results. BMMs were exposed to WT RANKL (2 μg/mL) or MT RANKL(2 μg/mL) at various time intervals after 8hrs with or without LiCl pretreatment.

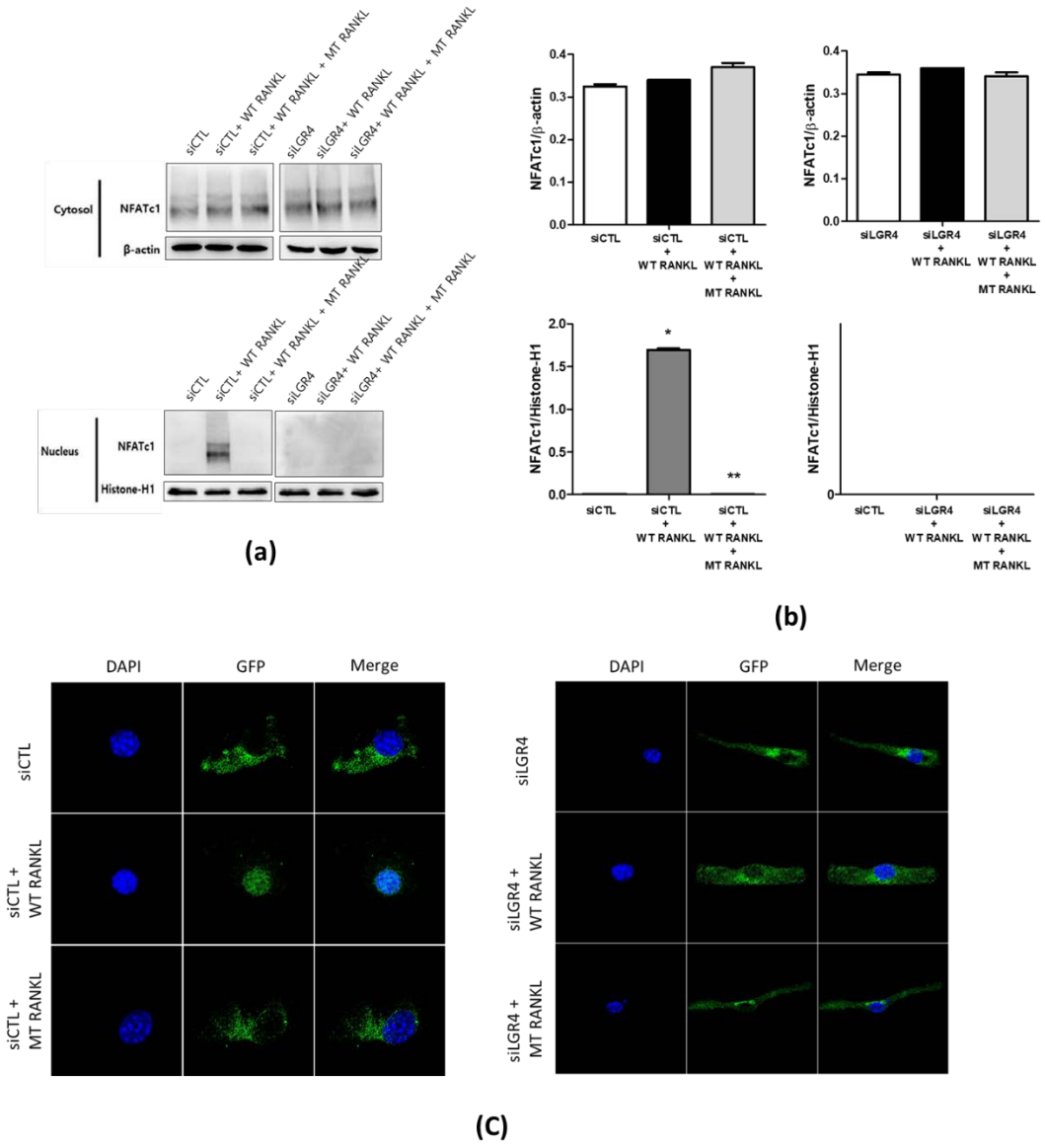

Figure 5. The effect of MT RANKL on NFATc1 translocation in LGR4 siRNA treated BMMs. (a) NFATc1 nuclear translocation was analyzed by western blot in the cytoplasmic and nuclear fractions. Histone-H1 and β-actin were used as loading controls for the nuclear and cytoplasmic fractions, respectively. (b) The densitometric analysis of NFATc1 in the cytoplasmic and nuclear fractions is

represented as the mean ratio ± standard deviation (SD) of three separate experiments. *P < 0.01, control group vs. WT RANKL ; **P < 0.01 WT RANKL vs.WT RANKL + MT RANKL. (c) NFATc1 nuclear translocation under confocal microscopy. Immunofluorescence images were acquired by staining for NFATc1 (green) and the nucleus (blue). Magnifications are 200X. Size bar is 20 μm.

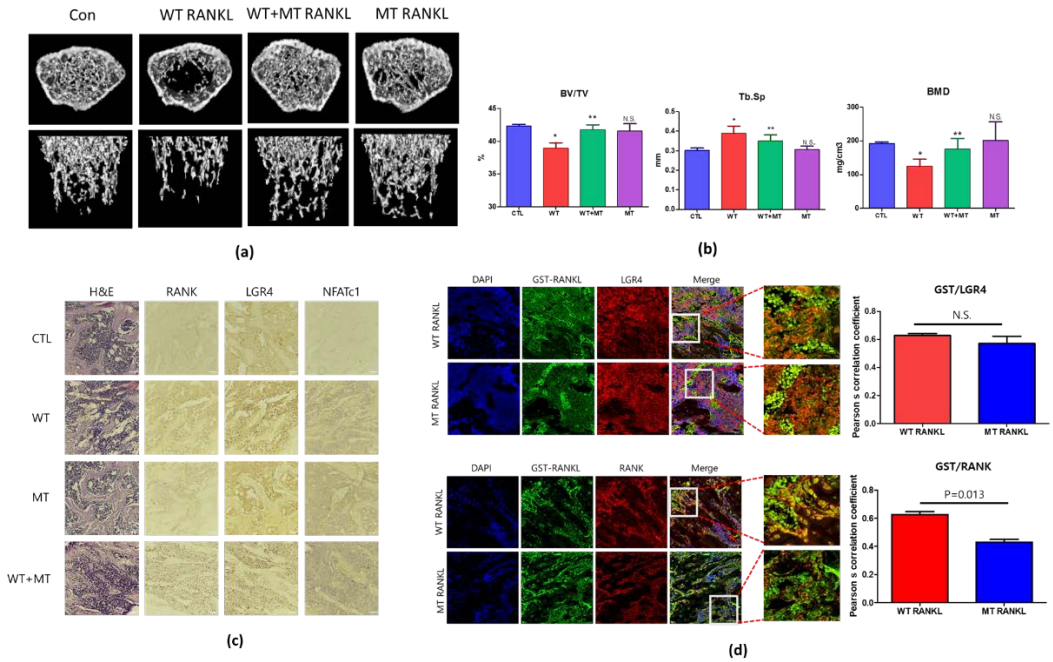

Figure 6. The effect of MT RANKL in vivo WT RANKL-induced mice model. (a) Representative micro-CT images of the distal femurs of mice. (b). Bone volume/total volume (BV/TV), trabecular thickness (Tb.Th), trabecular spacing (Tb/sp), Bone Volume (BV), Cortical thickness (Ct/Th), Bone Mineral Density (BMD). Values were expressed as means ± standard deviation (SD). (c) RANK and LGR4 IHC images of femurs. Magnifications are 200×. Size bar is 10 μm. (d) Confocal microscopy of RANK and LGR4 expression in WT RANKL or MT RANKL treated mice. Images were taken at 6309 magnification. Bar, 10 lm.